

This article was downloaded by:

On: 25 January 2011

Access details: *Access Details: Free Access*

Publisher *Taylor & Francis*

Informa Ltd Registered in England and Wales Registered Number: 1072954 Registered office: Mortimer House, 37-41 Mortimer Street, London W1T 3JH, UK



Liquid Crystals

Publication details, including instructions for authors and subscription information:

<http://www.informaworld.com/smpp/title~content=t713926090>

Novel hockey-stick mesogens with the nematic, synclonic and anticlinic smectic C phase sequence

Vladimíra Novotná^a; Jiří Žurek^b; Václav Kozmík^b; Jiří Svoboda^b; Milada Glogarová^a; Jan Kroupa^a; Damian Pocięcha^c

^a Institute of Physics, Academy of Science of the Czech Republic, Na Slovance 2, CZ-182 21 Prague 9, Czech Republic ^b Department of Organic Chemistry, Institute of Chemical Technology, CZ-166 28 Prague 6, Czech Republic ^c Laboratory of Dielectrics and Magnetics, Chemistry Department, Warsaw University, 02-089 Warsaw, Poland

To cite this Article Novotná, Vladimíra , Žurek, Jiří , Kozmík, Václav , Svoboda, Jiří , Glogarová, Milada , Kroupa, Jan and Pocięcha, Damian(2008) 'Novel hockey-stick mesogens with the nematic, synclonic and anticlinic smectic C phase sequence', *Liquid Crystals*, 35: 8, 1023 – 1036

To link to this Article: DOI: 10.1080/02678290802364012

URL: <http://dx.doi.org/10.1080/02678290802364012>

PLEASE SCROLL DOWN FOR ARTICLE

Full terms and conditions of use: <http://www.informaworld.com/terms-and-conditions-of-access.pdf>

This article may be used for research, teaching and private study purposes. Any substantial or systematic reproduction, re-distribution, re-selling, loan or sub-licensing, systematic supply or distribution in any form to anyone is expressly forbidden.

The publisher does not give any warranty express or implied or make any representation that the contents will be complete or accurate or up to date. The accuracy of any instructions, formulae and drug doses should be independently verified with primary sources. The publisher shall not be liable for any loss, actions, claims, proceedings, demand or costs or damages whatsoever or howsoever caused arising directly or indirectly in connection with or arising out of the use of this material.

Novel hockey-stick mesogens with the nematic, synclinc and anticlinc smectic C phase sequence

Vladimíra Novotná^b, Jiří Žurek^a, Václav Kozmík^a, Jiří Svoboda^{a*}, Milada Glogarová^b, Jan Kroupa^b and Damian Pocięcha^c

^aDepartment of Organic Chemistry, Institute of Chemical Technology, CZ-166 28 Prague 6, Czech Republic; ^bInstitute of Physics, Academy of Science of the Czech Republic, Na Slovance 2, CZ-182 21 Prague 9, Czech Republic; ^cLaboratory of Dielectrics and Magnetics, Chemistry Department, Warsaw University, Al. Zwirki i Wigury 101, 02-089 Warsaw, Poland

(Received 30 April 2008; final form 23 July 2008)

New hockey-stick mesogens have been synthesised and their mesomorphic properties studied. The molecular structure consists of a laterally substituted central naphthalene unit prolonged by two non-symmetrical arms, both of which contain ester units of identical orientation. The shorter arm possesses only one and the longer arm three benzene rings. Nematic, synclinc smectic C and anticlinc smectic C phases were identified and their physical properties studied. No banana-type ordering producing dipolar phases has been found.

Keywords: hockey-stick mesogen; synclinc smectic C phase; anticlinc smectic C phase

1. Introduction

Bent-shaped mesogens have become objects of considerable interest in the field of liquid crystal research in the past decade. Many different B-type phases have been recognised and characterised to date and their molecular structure–mesomorphic property relationships carefully investigated (1–13). Most of the studied material possess a central unit based on resorcinol and naphthalene-2,7-diol, ensuring a bent molecular structure, and the unit is usually connected to two identical arms. It has been shown that the mesomorphic properties can be broadly varied by lateral substitution of the central core, number of benzene units in the lengthening arms and their lateral substitution, type and length of the terminal group, etc.

Many non-symmetrical bent shaped mesogens have also been investigated. The non-symmetry of the molecular structure was introduced, for example, by different length and type of the terminal chain (14–23), by different functionalities in the central unit (14–16, 24–30), different number and lateral substitution of the benzene units in the arms (16, 18, 19, 27, 29–33), the type, number and orientation of the linking groups (28, 34–40), and combination of all these factors. A special sub-type of non-symmetrical bent-shaped liquid crystals are the hockey-stick mesogens, denomination of which was introduced for five-ring materials with non-symmetrical position of the bend (41). Thus, hockey-stick molecules are formed from a central core to which arms of a substantially different length are joined. For a three-ring bent molecule with only an aliphatic chain arm

the anticlinc smectic C (SmC_A) and synclinc smectic C (SmC_S) phases have been observed (42, 43). The nematic, SmC and SmC_A were formed in a structurally analogous four-ring system, and the antiferroelectric B2 phase was found in materials possessing polar linking groups in the lengthening arm (44). A bent-core 2,5-disubstituted 1,3,4-oxadiazole served also for design of luminiscent hockey-stick materials exhibiting standard calamitic nematic, smectic A (SmA), SmC and crystalline phases (45).

In previous research, we dealt with symmetrical and non-symmetrical five-ring bent-shaped mesogens based on a (laterally substituted) naphthalene-2,7-diol central core with ester and imino linking groups (46–49). All the compounds studied (46–49) have a similar length for both arms and variation of lateral substitution on the central naphthalene core. Ester group orientation and lengthening of the terminal chain led to formation a variety of B-type phases over a broad temperature interval. In addition, materials with a double bond in the terminal alkyl chain have been synthesised as model monomers for polymeric liquid crystals (22). In this paper, the synthesis and mesomorphic behaviour are reported of a series of novel hockey-stick mesogens based on a naphthalene-2,7-diol central core with a strongly non-symmetrical molecular shape, unlike common bent-shaped liquid crystals based on the same central core (42–45). The new compounds consist of a five-ring aromatic system connected with ester units of identical orientation. However, one arm of the novel mesogens possesses only one and the other three benzene rings, creating the typical hockey-stick profile.

*Corresponding author. Email: Jiri.Svoboda@vscht.cz

2. Experimental

Synthesis

To obtain the target materials (**I**) the arms were first prepared (Scheme 1). 4-Decyloxybenzoic (**1a**) and 4-dodecylbenzoic acids (**1b**) were obtained by a known method (50). To obtain the three-ring 4-(4-(4-alkoxybenzoyloxy)benzoyloxy)benzoic acids (**2a–2b**), a simple method was elaborated, different of that developed by Nozary *et al.* (51), starting with the frequently used two-ring acids **3a–3b** (52). In the first step, acids **3a–3b** were coupled with 4-hydroxybenzaldehyde in the presence of DCC and catalytic amount of 4-dimethylaminopyridine to esters **4a–4b** and the formyl group was oxidised in the next step with the Jones reagent in acetone to form acids **2a–2b** (Scheme 1).

Synthesis of compounds **1a–1c**.

Synthesis of the mesogen **1a** was performed by acylation of unsubstituted naphthalene-2,7-diol with freshly prepared acid chloride of **1b**. A three molar excess of naphthalene-2,7-diol and no base were used. At these conditions only a trace amount of diacylated product was formed and it was easily removed from the required 7-hydroxynaphthyl ester **5a** by column chromatography. In the next step, hydroxy ester **5a** was esterified with acid **2a** by a standard DCC-mediated esterification method (Scheme 2).

For the synthesis of non-symmetrical laterally 1-substituted naphthalene-2,7-diol-based mesogens we used a methodology described previously (22). The starting *tert*-butyldimethylsilyl (TBDMS)-protected 1-substituted naphthalene-2,7-diols (22) were

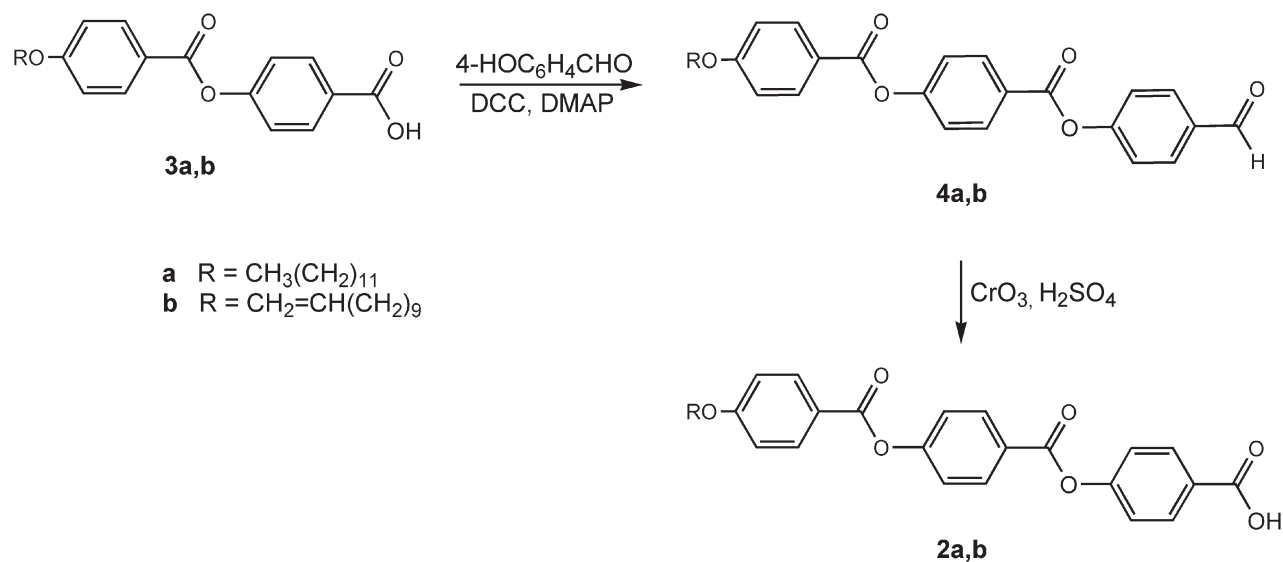
obtained by a selective silylation of the corresponding 1-methyl-, 1-chloro- and 1-cyano-naphthalene-2,7-diols with TBDMS-Cl. The methyl-substituted mesogen **1b** was then obtained by esterification of **6b** first with acid **1b** by the DCC method to afford the protected ester **7b** (Scheme 3). Deprotection of the silyl group was achieved with tetrabutylammonium fluoride and the formed 7-hydroxynaphthyl ester **5b** was further acylated analogously with acid **2a** to give rise to **1b**. When reversing the sequence of successive esterifications, i.e. first the reaction of **6b** with acid **2a** and the formed intermediate **7c** second with acid **1b**, the isomeric material **1c** could also be obtained.

Synthesis of compounds **1d–1f**.

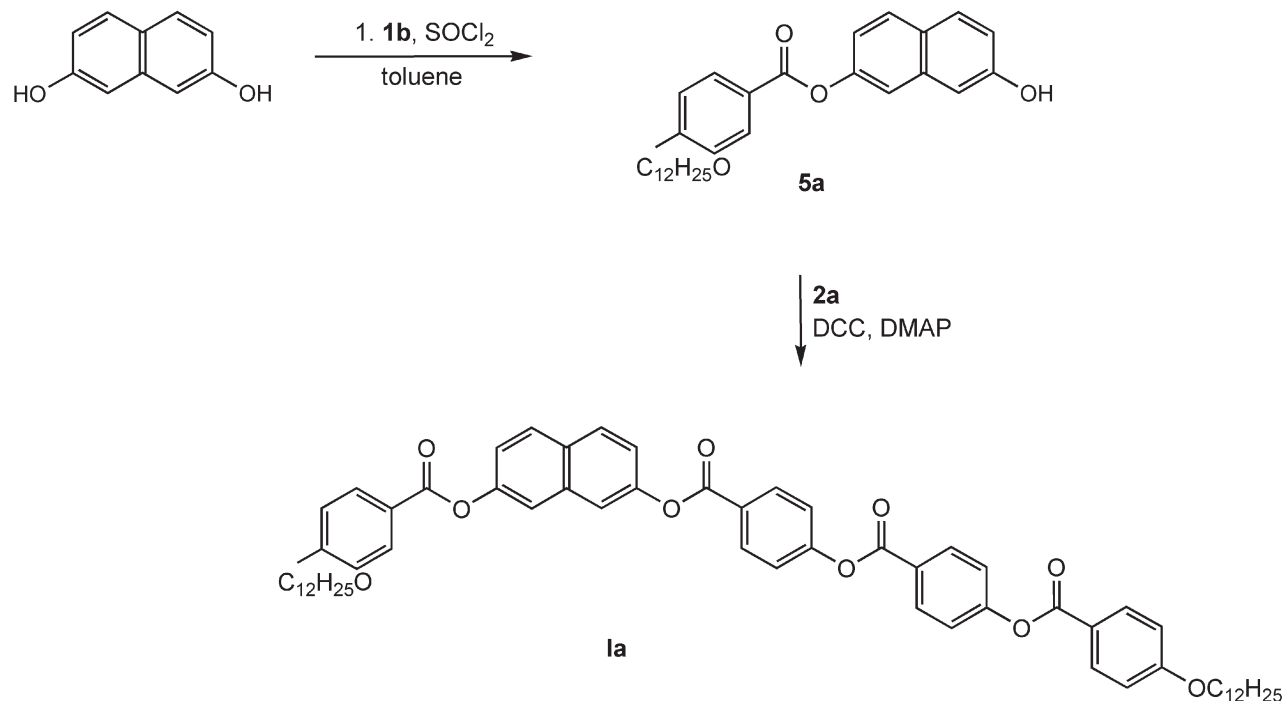
In the same way, materials **1d–1f** were obtained starting with **6b**, 2-silyl-protected 8-chloro- (**6e**) and 8-cyanonaphthalene-2,7-diols (**6f**) (22), and acids **1a** and **2b** (Scheme 4). Isolation, characterisation, and purification of all intermediates and products are summarised in the following section.

Characterisation

Confirmation of the structures of intermediates and products was obtained by ¹H NMR spectroscopy (Varian Gemini 300 HC instrument; CDCl₃ was used as solvent and signals of the solvent served as internal standard; *J* values are given in Hz). Elemental analyses were carried out on a Perkin-Elmer 2400 instrument. The purity of all final compounds was checked by HPLC analysis (Tessek C18 25 × 4.5 RP column) and found to be >99.8%. Column chromatography was carried out using Merck Kieselgel 60



Scheme 1. Synthesis of the three-ring acids **2a**, **2b**.

Scheme 2. Synthesis of the parent hockey-stick mesogen **1a**.

(60–100 μm). The experimental section summarises procedures for the synthesis of representative intermediates and target compounds of series **I**.

(4-Formylphenyl) 4-(4-(dodecyloxy)benzoyloxy)benzoate (4a).

To a solution of acid **3a** (1.0 g, 2.34 mmol), 4-hydroxybenzaldehyde (0.268 g, 2.35 mmol), and DMAP (7 mg) in dry dichloromethane (20 ml) was added DCC (0.642 g, 3.11 mmol) in argon atmosphere. The mixture was stirred at room temperature for 2 h, decomposed with water (2 ml) and after stirring for 30 min filtered and the solid washed with dichloromethane (2 \times 10 ml). The organic solution was washed with brine (20 ml), dried with anhydrous magnesium sulfate and evaporated. The residue was purified by column chromatography (silica gel, elution with toluene/*tert*-butyl methyl ether 12/1). 1.19 g (96%) of ester **4a** was obtained, m.p. 105°C. $^1\text{H NMR}$: 0.88 (t, 3 H, CH_3), 1.00–1.60 (m, 18 H, $(\text{CH}_2)_9$), 1.83 (m, 2 H, CH_2), 4.05 (t, 2 H, CH_2O), 6.99 (d, 2 H, $^3J=8.8$, H-3, H-5), 7.39 (d, 2 H, $^3J=8.8$, H-3, H-5), 7.42 (d, 2 H, $^3J=8.8$, H-3, H-5), 7.99 (d, 2 H, H-2, H-6), 8.15 (d, 2 H, H-2, H-6), 8.28 (d, 2 H, H-2, H-6), 10.04 (s, 1 H, CHO). Elemental analysis for $\text{C}_{33}\text{H}_{38}\text{O}_6$ (530.67): calculated C 74.69, H 7.22; found C 74.55, H 7.11%.

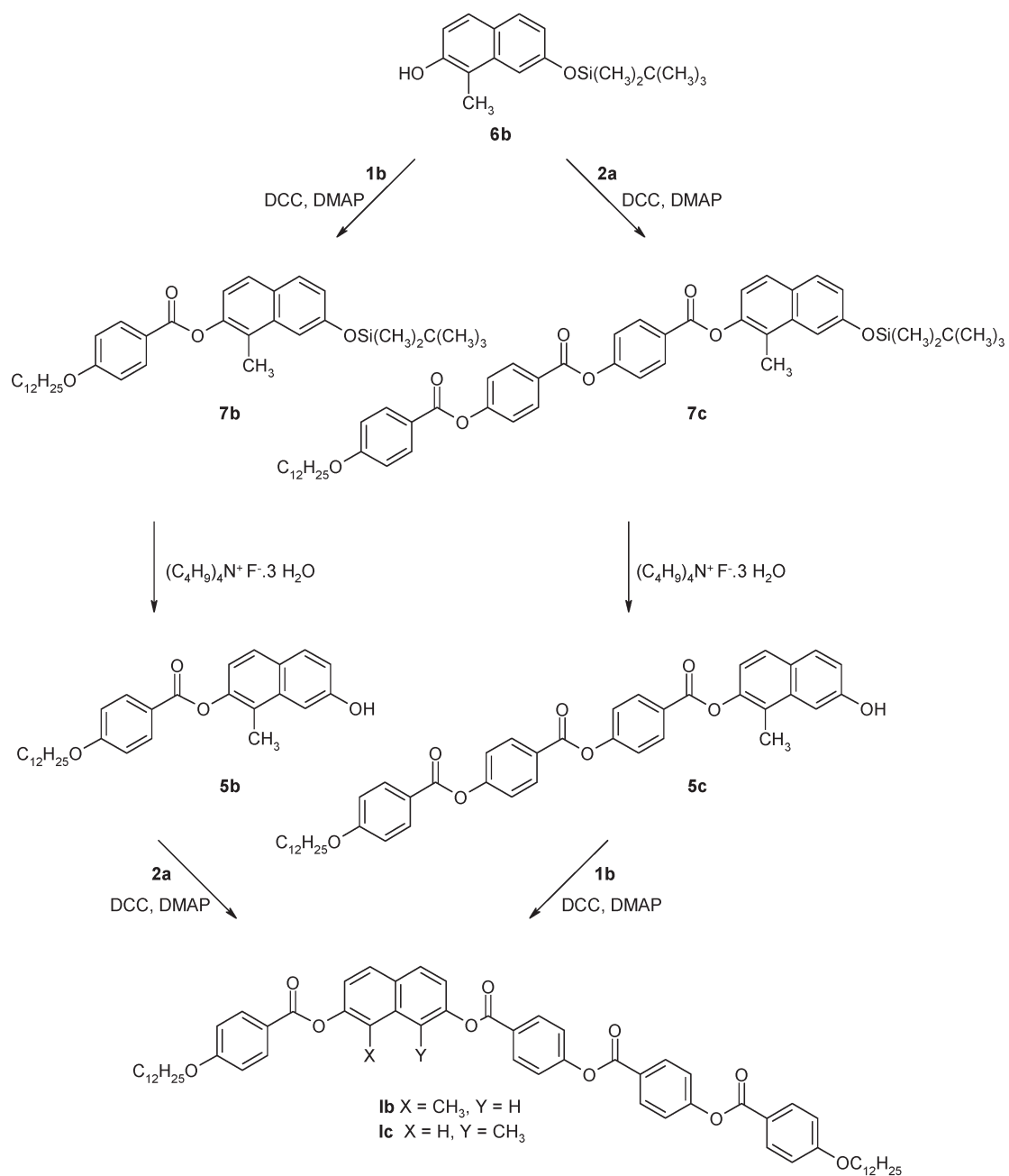
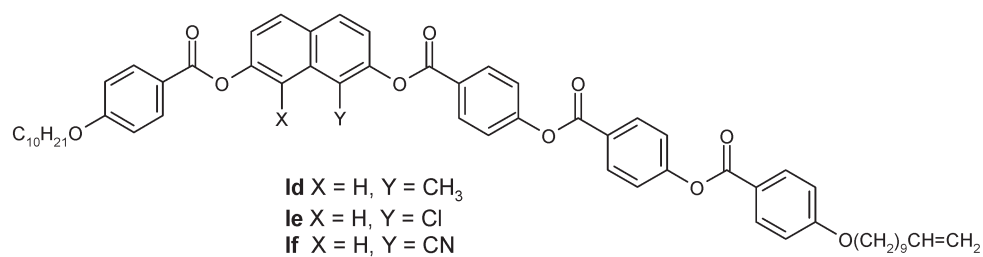
In the same way starting with acid **3b**, ester **4b** was obtained in 84% yield, m.p. 84°C. $^1\text{H NMR}$: 1.00–1.55 (m, 14 H, $(\text{CH}_2)_7$), 1.83 (m, 2H, CH_2), 4.05 (t,

2H, CH_2O), 4.96 (m, 2 H, $\text{CH}_2=$), 5.83 (m, 1 H, =CH), 6.99 (d, 2 H, $^3J=8.8$, H-3, H-5), 7.39 (d, 2 H, $^3J=8.8$, H-3, H-5), 7.43 (d, 2 H, $^3J=8.8$, H-3, H-5), 7.99 (d, 2 H, H-2, H-6), 8.15 (d, 2 H, H-2, H-6), 8.28 (d, 2 H, H-2, H-6), 10.03 (s, 1 H, CHO). Elemental analysis for $\text{C}_{32}\text{H}_{34}\text{O}_6$ (514.62): calculated C 74.69, H 6.66; found C 74.49, H 6.49%.

4-(4-(4-(Dodecyloxy)benzoyloxy)benzoyloxy)benzoic acid (2a).

To a solution of formyl compound **4a** (1.152 g, 2.17 mmol) in acetone (35 ml) was added dropwise the Jones reagent (1.74 ml) at 0–5°C, then the mixture was stirred at room temperature for 2.5 h and poured on water (200 ml). The precipitate was filtered, washed with water and dried. Crystallisation from toluene afforded 1.082 g (92%) of acid **2a**, m.p. 188–189°C [m.p. (51) 171–173°C]. $^1\text{H NMR}$: 0.88 (t, 3 H, CH_3), 1.10–1.65 (m, 18 H, $(\text{CH}_2)_9$), 1.83 (m, 2 H, CH_2), 4.05 (t, 2 H, CH_2O), 6.99 (d, 2 H, $^3J=8.8$, H-3, H-5), 7.36 (d, 2 H, $^3J=8.8$, H-3, H-5), 7.39 (d, 2 H, $^3J=8.8$, H-3, H-5), 8.16 (d, 2 H, H-2, H-6), 8.20 (d, 2 H, H-2, H-6), 8.29 (d, 2 H, H-2, H-6). Elemental analysis for $\text{C}_{33}\text{H}_{38}\text{O}_7$ (546.67): calculated C 72.51, H 7.01; found C 72.50, H 6.94%.

Analogously acid **2b** was prepared (97% yield), m.p. 177–179°C. $^1\text{H NMR}$: 1.20–1.60 (m, 14 H, $(\text{CH}_2)_7$), 1.83 (m, 2H, CH_2), 4.05 (t, 2H, CH_2O), 4.96 (m, 2 H, $\text{CH}_2=$), 5.83 (m, 1 H, =CH), 7.10 (d, 2 H,

Scheme 3. Synthesis of the isomeric methyl-substituted materials **Ib**, **Ic**.Scheme 4. Structure of the monomeric materials **Id–If**.

$^3J=8.8$, H-3, H-5), 7.43 (d, 2 H, $^3J=8.8$, H-3, H-5), 7.51 (d, 2 H, $^3J=8.8$, H-3, H-5), 8.03 (d, 2 H, H-2, H-6), 8.08 (d, 2 H, H-2, H-6), 8.22 (d, 2 H, H-2, H-6). Elemental analysis for $C_{32}H_{34}O_7$ (530.62): calculated C 72.43, H 6.46; found C 72.20, H 6.40%.

(7-Hydroxynaphthalen-2-yl) 4-(dodecyloxy)benzoate (5a).

To a mixture of acid **1b** (2.0 g, 6.5 mmol), one drop of pyridine, and toluene (100 ml), thionyl chloride (2.2 g, 18.4 mmol) was added and the solution was heated to boiling for 4 h and evaporated. The crude acid chloride was dissolved in toluene (10 ml) and added dropwise to a boiling solution of naphthalene-2,7-diol (3.14 g, 19.6 mmol) in toluene (50 ml). The heating was continued for 4 h, then the mixture was cooled to room temperature and decomposed with water (150 ml). The organic layer was separated and the aqueous layer was extracted with dichloromethane (3×60 ml). The combined organic solution was washed with water (50 ml) and brine (50 ml). After evaporation the product was purified by column chromatography (silica gel, elution with toluene/*tert*-butyl methyl ether 12/1). 75 mg (1.6%) of naphthalene-2,7-diyl bis(4-dodecyloxy)benzoate, and 2.08 g (71%) of **5a** were isolated, m.p. 105.5–107°C. 1H NMR: 0.88 (t, 3 H, CH_3), 1.20–1.60 (m, 18 H, $(CH_2)_9$), 1.83 (m, 2 H, CH_2), 4.05 (t, 2 H, CH_2O), 5.20 s (1 H, OH), 6.98 (d, 2 H), 7.04 dd (1 H, $^3J=8.8$, $^4J=2.1$, H-6), 7.06 (d, 1 H, H-8), 7.16 dd (1 H, $^3J=8.8$, $^4J=2.1$, H-3), 7.47 (d, 1 H, H-1), 7.72 (d, 1 H, H-5), 7.78 (d, 1 H, H-4), 8.18 (d, 2 H). Elemental analysis for $C_{29}H_{36}O_4$ (448.61): calculated C 77.65, H 8.09; found C 77.42, H 8.01%.

General esterification procedure.

A mixture of the corresponding hydroxy derivative (1.0 mmol), acid (1.25 mmol), DCC (1.5 mmol) and catalytic amount of DMAP in dry dichloromethane (50 ml) was stirred at room temperature in argon atmosphere for 2 h. The excess of DCC was decomposed with water (0.5 ml), the mixture was filtered and the solid washed with dichloromethane (2×10 ml). The combined filtrate was evaporated and purified.

(7-(tert-Butyldimethylsilyloxy)-1-methylnaphthalen-2-yl) 4-(dodecyloxy)benzoate (7b) was obtained by the reaction of **6b** and **1b**. Purification by column chromatography (silica gel, elution with hexane/ethyl acetate 6/1), yield 82%, m.p. 98–99°C. 1H NMR: 0.26 s (6 H, $(CH_3)_2Si$), 0.88 (t, 3 H, CH_3), 1.03 s (9 H, $(CH_3)_3C$), 1.20–1.60 (m, 18 H, $(CH_2)_9$), 1.83 (m, 2 H, CH_2), 2.45 s (3 H, CH_3), 4.06 (t, 2 H, CH_2O), 7.00 (d, 2

H), 7.07 dd (1 H, $^3J=8.8$, $^4J=2.1$, H-6), 7.13 (d, 1 H, H-3), 7.34 (d, 1 H, $^4J=2.1$, H-8), 7.67 (d, 1 H, H-5), 7.73 (d, 1 H, H-4), 8.21 (d, 2 H). Elemental analysis for $C_{36}H_{52}O_4Si$ (576.90): calculated C 74.95, H 9.09; found C 74.66, H 8.88%.

(7-(tert-Butyldimethylsilyloxy)-1-methylnaphthalen-2-yl) 4-(4-(4-(dodecyloxy)benzoyloxy)benzoyloxy)benzoate (7c) was obtained from **6b** and **2a**. Purification was performed by column chromatography (silica gel, elution with chloroform), yield 52%, m.p. 128–129.5°C. 1H NMR: 0.27 s (6 H, $(CH_3)_2Si$), 0.89 (t, 3 H, CH_3), 1.03 s (9 H, $(CH_3)_3C$), 1.20–1.60 (m, 18 H, $(CH_2)_9$), 1.83 (m, 2 H, CH_2), 2.47 s (3 H, CH_3), 4.06 (t, 2 H, CH_2O), 6.99 (d, 2 H), 7.09 dd (1 H, $^3J=8.8$, $^4J=2.0$, H-6), 7.15 (d, 1 H, $^3J=8.8$, H-3), 7.37 (d, 1 H, $^4J=2.0$, H-8), 7.40 (d, 2 H), 7.42 (d, 2 H), 7.70 (d, 1 H, $^3J=8.8$, H-5), 7.75 (d, 1 H, H-4), 8.16 (d, 2 H), 8.31 (d, 2 H), 8.37 (d, 2 H). Elemental analysis for $C_{50}H_{60}O_8Si$ (817.12) calculated C 73.50, H 7.40; found C 73.22, H 7.19%.

(7-(tert-Butyldimethylsilyloxy)-1-methylnaphthalen-2-yl) 4-(4-(4-(undec-10-enyloxy)benzoyloxy)benzoyloxy)benzoate (7d) resulted from the reaction **6b** and acid **2b**. Purification was performed by column chromatography (silica gel, elution with chloroform), yield 51%, m.p. 140–140.5°C. 1H NMR: 0.27 s (6 H, $(CH_3)_2Si$), 1.03 s (9 H, $(CH_3)_3C$), 1.20–1.65 (m, 12 H, $(CH_2)_6$), 1.83 (m, 2 H, CH_2), 2.05 q (2 H, CH_2), 2.48 s (3 H, CH_3), 4.07 (t, 2 H, CH_2O), 4.98 (m, 2 H, $CH_2=$), 5.82 (1 H, =CH), 7.00 (d, 2 H), 7.08 dd (1 H, $^3J=8.8$, $^4J=2.0$, H-6), 7.15 (d, 1 H, $^3J=8.8$, H-3), 7.37 (d, 1 H, $^4J=2.0$, H-8), 7.41 (d, 2 H), 7.42 (d, 2 H), 7.70 (d, 1 H, $^3J=8.8$, H-5), 7.75 (d, 1 H, H-4), 8.17 (d, 2 H), 8.31 (d, 2 H), 8.37 (d, 2 H). Elemental analysis for $C_{49}H_{56}O_8Si$ (801.07) calculated C 73.47, H 7.05; found C 73.35, H 6.96%.

(7-(tert-Butyldimethylsilyloxy)-8-chloronaphthalen-2-yl) 4-(decyloxy)benzoate (7e) was obtained by acylation of **6e** with **1a**. Purification by column chromatography (silica gel, elution with 1,2-dichloroethane), yield 76%, oil. 1H NMR: 0.27 s (6 H, $(CH_3)_2Si$), 0.89 (t, 3 H, CH_3), 1.08 s (9 H, $(CH_3)_3C$), 1.20–1.55 (m, 14 H, $(CH_2)_7$), 1.83 (m, 2 H, CH_2), 4.06 (t, 2 H, CH_2O), 6.99 (d, 2 H), 7.12 (d, 1 H, $^3J=8.8$, H-6), 7.28 dd (1 H, $^3J=8.8$, $^4J=2.1$, H-3), 7.67 (d, 1 H, $^3J=8.8$, H-5), 7.82 (d, 1 H, H-4), 8.00 (d, 1 H, H-1), 8.19 (2 H). Elemental analysis for $C_{33}H_{45}ClO_4Si$ (569.26): calculated C 69.63, H 7.97, Cl 6.23; found C 69.44, H 7.79, Cl 6.08%.

(7-(tert-Butyldimethylsilyloxy)-8-cyanonaphthalen-2-yl) 4-(decyloxy)benzoate (7f) was obtained by the reaction of **6f** and **1a**. Purification by column chromatography (silica gel, elution with toluene/*tert*-butyl methyl ether 20/1), yield 88%, m.p. 80–90°C. 1H NMR: 0.28 s (6 H, $(CH_3)_2Si$), 0.88 (t, 3 H, CH_3), 1.08 s (9 H, $(CH_3)_3C$), 1.20–1.60 (m, 14 H, $(CH_2)_7$), 1.83 (m,

2 H, CH₂), 4.06 (t, 2 H, CH₂O), 6.99 (d, 2 H), 7.07 (d, 1 H, ³J=8.8, H-6), 7.27 (d, 1 H, H-1), 7.36 dd (1 H, ³J=8.8, ⁴J=2.1, H-3), 7.87 (d, 1 H, H-4), 7.93 (d, 1 H, ³J=8.8, H-5), 8.17 (2 H). Elemental analysis for C₃₄H₄₅NO₄Si (559.83): calculated C 72.95, H 8.10, N 2.50; found C 72.77, H 7.93, N 2.33%.

(7-Hydroxy-1-methylnaphthalen-2-yl) 4-(dodecyloxy) benzoate (**5b**).

Bu₄N⁺F⁻·3H₂O (26 mg, 0.085 mmol) was added to a solution of silyl ester **7b** (192 mg, 0.333 mmol) in a mixture of THF (15 ml) and water (0.5 ml) and the mixture was stirred at room temperature for 15 min. Another portion of Bu₄N⁺F⁻·3H₂O (26 mg; 0.085 mmol) was added, and stirring was continued for 10 min. The solution was diluted with water (25 ml) and extracted with ethyl acetate (3 × 30 ml), the combined organic solution was washed with water (20 ml), brine (20 ml), and dried with anhydrous magnesium sulfate. After evaporation of the solvent the crude product was purified by column chromatography on silica gel (elution with hexane/ethyl acetate 4/1). Yield 145 mg (97%), m.p. 119–121°C. ¹H NMR: 0.88 (t, 3 H, CH₃), 1.20–1.60 (m, 18 H, (CH₂)₉), 1.83 (m, 2 H, CH₂), 2.44 s (3 H, CH₃), 4.06 (t, 2 H, CH₂O), 5.04 s (1 H, OH), 7.00 (d, 2 H, ³J=8.8), 7.07 dd (1 H, ³J=8.8, ⁴J=2.3, H-6), 7.13 (d, 1 H, ³J=8.8, H-3), 7.29 (d, 1 H, H-8), 7.67 (d, 1 H, H-5), 7.75 (d, 1 H, H-4), 8.21 (d, 2 H). Elemental analysis for C₃₀H₃₈O₄ (462.63): calculated C 77.89, H 8.28; found C 77.71, H 8.17%.

In the same way, by deprotection of **7c–7f**, hydroxy esters **5c–5f** were obtained.

For (7-hydroxy-1-methylnaphthalen-2-yl) 4-(4-(4-(dodecyloxy)benzoyloxy)-benzoyloxy)benzoate (**5c**), purification was by column chromatography (silica gel, elution with toluene/*tert*-butyl methyl ether 12/1), yield 83%, m.p. 136–137°C. ¹H NMR: 0.88 (t, 3 H, CH₃), 1.15–1.60 (m, 18 H, (CH₂)₉), 1.83 (m, 2 H, CH₂), 2.46 s (3 H, CH₃), 4.06 (t, 2 H, CH₂O), 5.12 s (1 H, OH), 6.99 (d, 2 H), 7.10 dd (1 H, ³J=8.8, ⁴J=2.1, H-6), 7.15 (d, 1 H, ³J=8.8, H-3), 7.31 (d, 1 H, ⁴J=2.1, H-8), 7.40 (d, 2 H), 7.42 (d, 2 H), 7.70 (d, 1 H, ³J=8.8, H-5), 7.77 (d, 1 H, H-4), 8.16 (d, 2 H), 8.31 (d, 2 H), 8.37 (d, 2 H). Elemental analysis for C₄₄H₄₆O₈ (702.85): calculated C 75.19, H 6.60; found C 75.10, H 6.52%.

For (7-hydroxy-1-methylnaphthalen-2-yl) 4-(4-(4-(undec-10-enyloxy)benzoyloxy)-benzoyloxy)benzoate (**5d**), purification was by column chromatography (silica gel, elution with toluene/*tert*-butyl methyl ether 20/1), yield 64%, m.p. 169–170°C. ¹H NMR: 1.10–1.55 (m, 12 H, (CH₂)₆), 1.83 (m, 2 H, CH₂), 2.05 q (2 H, CH₂), 2.46 s (3 H, CH₃), 4.06 (t, 2 H, CH₂O),

5.17 s (1 H, OH), 4.97 (m, 2 H, CH₂=), 5.82 (1 H, =CH), 7.00 (d, 2 H), 7.09 dd (1 H, ³J=8.8, ⁴J=2.1, H-6), 7.15 (d, 1 H, ³J=8.8, H-3), 7.31 (d, 1 H, ⁴J=2.5, H-8), 7.41 (d, 2 H), 7.42 (d, 2 H), 7.70 (d, 1 H, ³J=8.8, H-5), 7.77 (d, 1 H, H-4), 8.17 (d, 2 H), 8.31 (d, 2 H), 8.37 (d, 2 H). Elemental analysis for C₄₃H₄₂O₈ (686.81): calculated C 75.20, H 6.16; found C 75.11, H 6.175.

For (8-chloro-7-hydroxynaphthalen-2-yl) 4-(decyloxy)benzoate (**5e**), purification was performed by column chromatography (silica gel, elution with dichloromethane), yield 64%, m.p. 170–171°C. ¹H NMR: 0.89 (t, 3 H, CH₃), 1.20–1.60 (m, 14 H, (CH₂)₇), 1.83 (m, 2 H, CH₂), 4.06 (t, 2 H, CH₂O), 5.91 s (1 H, OH), 6.99 (d, 2 H), 7.25 (d, 1 H, ³J=8.8, H-6), 7.27 dd (1 H, ³J=8.8, ⁴J=2.1, H-3), 7.73 (d, 1 H, ³J=8.8, H-5), 7.84 (d, 1 H, H-4), 7.87 (d, 1 H, H-1), 8.19 (2 H). Elemental analysis for C₂₇H₃₁ClO₄ (455.00): calculated C 71.28, H 6.87, Cl 7.79; found C 71.15, H 6.69, Cl 7.72%.

For (8-cyano-7-hydroxynaphthalen-2-yl) 4-(decyloxy)benzoate (**5f**), purification was by column chromatography (silica gel, elution with dichloromethane), yield 83%, m.p. 136–137°C. ¹H NMR: 0.89 (t, 3 H, CH₃), 1.15–1.65 (m, 14 H, (CH₂)₇), 1.83 (m, 2 H, CH₂), 4.06 (t, 2 H, CH₂O), 5.19 s (1 H, OH), 7.01 (d, 2 H), 7.06 (d, 1 H, ³J=8.8, H-6), 7.30 dd (1 H, ³J=8.8, ⁴J=2.2, H-3), 7.73 (d, 1 H, H-1), 7.89 (d, 1 H, H-4), 7.94 (d, 1 H, ³J=8.8, H-5), 8.19 (2 H). Elemental analysis for C₂₈H₃₁NO₄ (445.56): calculated C 75.48, H 7.01, N 3.14; found C 75.35, H 6.86, N 3.02%.

(7-(4-(4-(4-(Dodecyloxy)benzoyloxy)benzoyloxy)benzoyloxy)naphthalen-2-yl) 4-(dodecyloxy)benzoate (**1a**).

A mixture of **5a** (449 mg, 1 mmol), acid **2a** (683 mg, 1.25 mmol), DCC (309 mg, 1.5 mmol) and DMAP (7 mg) in dry dichloromethane (50 ml) was stirred for 2 h at room temperature in argon atmosphere. Water (0.5 ml) was added, the mixture was stirred for 30 min and the precipitated *N,N'*-dicyclohexylurea was filtered off and washed with dichloromethane (20 ml). The filtrate was evaporated and the residue was purified by column chromatography (silica gel, elution with 1,2-dichloroethane) and crystallised from toluene to afford 605 mg (62%) of **1a**. ¹H NMR: 0.88 (t, 6 H, 2 CH₃), 1.20–1.60 (m, 36 H, 2 (CH₂)₉), 1.83 (m, 4 H, 2 CH₂), 4.05 (t, 4 H, 2 × CH₂), 6.99 (d, 4 H, ³J=8.8), 7.35–7.43 (m, 2 H), 7.40 (d, 2 H), 7.42 (d, 2 H), 7.68 (d, 2 H), 7.93 (d, 2 H), 8.16 (d, 2 H), 8.19 (d, 2 H), 8.31 (d, 2 H), 8.35 (d, 2 H). Elemental analysis for C₆₂H₇₂O₁₀ (977.26): calculated C 76.20, H 7.43; found C 75.93, H 7.38%.

(7-(4-Dodecyloxy)benzoyloxy)-8-methylnaphthalen-2-yl) 4-(4-(4-(dodecyloxy)-benzoyloxy)benzoyloxy)benzoate (**1b**) was obtained from **5b** and acid **2a**. Purification by column chromatography (silica gel, elution with 1,2-dichloroethane) and crystallisation from toluene, yield 65%. $^1\text{H NMR}$: 0.88 (t, 6 H, CH_3), 1.15–1.60 (m, 36 H, $2 \times (\text{CH}_2)_9$), 1.83 (m, 4 H, $2 \times \text{CH}_2$), 2.53 s (3 H, CH_3), 4.06 (t, 4 H, $2 \times \text{CH}_2\text{O}$), 6.99 (d, 2 H), 7.00 (d, 2 H), 7.30 (d, 1 H, $^3J=8.8$, H-6), 7.37 dd (1 H, $^3J=8.8$, $^4J=2.0$, H-3), 7.40 (d, 2 H), 7.42 (d, 2 H), 7.80 (d, 1 H, H-5), 7.85 (d, 1 H, H-1), 7.94 (d, 1 H, H-4), 8.16 (d, 2 H), 8.22 (d, 2 H), 8.31 (d, 2 H), 8.36 (d, 2 H). Elemental analysis for $\text{C}_{63}\text{H}_{74}\text{O}_{10}$ (991.29): calculated C 76.34, H 7.52; found C 76.19, H 7.395.

((7-(4-Dodecyloxy)benzoyloxy)-1-methylnaphthalen-2-yl) 4-(4-(4-(dodecyloxy)-benzoyloxy)benzoyloxy)benzoate (**1c**) was obtained by acylation of **5c** with **1b**. Purification by column chromatography (silica gel, elution with 1,2-dichloroethane) and crystallisation from toluene, yield 77%. $^1\text{H NMR}$: 0.88 (t, 6 H, CH_3), 1.20–1.60 (m, 36 H, $2 (\text{CH}_2)_9$), 1.83 (m, 4 H, 2CH_2), 2.53 s (3 H, CH_3), 4.06 (t, 4 H, $2 \text{CH}_2\text{O}$), 6.99 (d, 2 H), 7.00 (d, 2 H), 7.30 (d, 1 H, $^3J=9.0$, H-3), 7.38 dd (1 H, $^3J=8.8$, $^4J=2.0$, H-6), 7.40 (d, 2 H), 7.43 (d, 2 H), 7.81 (d, 1 H, H-4), 7.84 (d, 1 H, H-8), 7.93 (d, 1 H, H-5), 8.16 (d, 2 H), 8.21 (d, 2 H), 8.31 (d, 2 H), 8.38 (d, 2 H). Elemental analysis for $\text{C}_{63}\text{H}_{74}\text{O}_{10}$ (991.29): calculated C 76.34, H 7.52; found C 76.25, H 7.43%.

(7-(4-(Decyloxy)benzoyloxy)-1-methylnaphthalen-2-yl) 4-(4-(4-(undec-10-enyloxy)-benzoyloxy)benzoyloxy)benzoate (**1d**) resulted from **5f** and acid **2b**. Purification was by column chromatography (silica gel, elution with 1,2-dichloroethane) and crystallisation from cyclohexane, yield 81%. $^1\text{H NMR}$: 0.89 (t, 3 H, CH_3), 1.10–1.55 (m, 36 H, $(\text{CH}_2)_n$), 1.83 (m, 2 H, CH_2), 2.05 (m, 2 H, CH_2), 2.53 s (3 H, CH_3), 4.06 (t, 2 H, CH_2O), 4.97 (m, 2 H, $\text{CH}_2=$), 5.82 (1 H, $=\text{CH}$), 7.00 (d, 4 H), 7.31 (d, 1 H, $^3J=8.7$, H-3), 7.38 dd (1 H, $^3J=8.0$, $^4J=2.1$, H-6), 7.41 (d, 2 H), 7.43 (d, 2 H), 7.81 (d, 1 H, $^3J=9.0$, H-4), 7.84 (d, 1 H, $^4J=2.1$, H-8), 7.93 (d, 1 H, H-5), 8.16 (d, 2 H), 8.31 (d, 4 H), 8.38 (d, 2 H). Elemental analysis for $\text{C}_{60}\text{H}_{66}\text{O}_{10}$ (947.19): calculated C 76.09, H 7.02; found C 75.95, H 6.87%.

(8-Chloro-7-(4-(4-(4-(undec-10-enyloxy)benzoyloxy)benzoyloxy)benzoyloxy)-naphthalen-2-yl) 4-(decyloxy)benzoate (**1e**) resulted from **5e** and acid **2b**. Purification was by column chromatography (silica gel, elution with toluene/*tert*-butyl methyl ether 12/1) and crystallisation from cyclohexane, yield 62%. $^1\text{H NMR}$: 0.89 (t, 3 H, CH_3), 1.15–1.60 (m, 26 H, $(\text{CH}_2)_n$), 1.83 (m, 2 H, CH_2), 2.05 (m, 2 H, CH_2), 4.06 (t, 2 H, CH_2O), 4.95 (m, 2 H, $\text{CH}_2=$), 5.82 (1 H, $=\text{CH}$), 7.00 (d, 4 H), 7.40 (d, 2 H), 7.42 (d, 2 H), 7.44 (d, 1 H, $^3J=8.8$, H-3), 7.46 dd

(1 H, $^3J=8.8$, $^4J=1.8$, H-6), 7.88 (d, 1 H, $^3J=9.0$, H-4), 7.96 (d, 1 H, H-5), 8.12 (d, 1 H, $^4J=1.8$, H-8), 8.16 (d, 2 H), 8.20 (d, 2 H), 8.31 (d, 2 H), 8.40 (d, 2 H). Elemental analysis for $\text{C}_{59}\text{H}_{63}\text{ClO}_{10}$ (967.61): calculated C 73.24, H 6.56, Cl 3.66; found C 73.22, H 6.62, Cl 3.44%.

(8-Cyano-7-(4-(4-(4-(undec-10-enyloxy)benzoyloxy)benzoyloxy)benzoyloxy)naphthalen-2-yl) 4-(decyloxy)benzoate (**1f**) was obtained by acylation of **5f** with acid **2b**. Purification by column chromatography (silica gel, elution with dichloromethane) and crystallisation from 1,2-dichloroethane, yield 76%. $^1\text{H NMR}$: 0.89 (t, 3 H, CH_3), 1.10–1.80 (m, 26 H, $(\text{CH}_2)_n$), 1.83 (m, 2 H, CH_2), 2.05 (m, 2 H, CH_2), 4.07 (t, 2 H, CH_2O), 4.95 (m, 2 H, $\text{CH}_2=$), 5.82 (1 H, $=\text{CH}$), 6.99 (d, 2 H), 7.01 (d, 2 H), 7.40 (d, 2 H), 7.45 (d, 2 H), 7.55 dd (1 H, $^3J=8.8$, $^4J=2.0$, H-6), 7.59 (d, 1 H, $^3J=9.0$, H-3), 8.02 (d, 1 H, H-5), 8.05 (d, 1 H, H-8), 8.16 (d, 1 H, $^3J=9.0$, H-4), 8.16 (d, 2 H), 8.21 (d, 2 H), 8.31 (d, 2 H), 8.38 (d, 2 H). Elemental analysis for $\text{C}_{30}\text{H}_{63}\text{NO}_{10}$ (958.17): calculated C 75.21, H 6.63, N 1.46; found C 75.09, H 6.44, N 1.33.

Experimental methods

All materials were studied using differential scanning calorimetry (DSC, Perkin–Elmer Pyris Diamond). The samples, 2–4 mg, were hermetically closed in aluminium pans and placed in a nitrogen atmosphere. Cooling and heating rates of 5 K min^{-1} were applied.

Texture observations were carried out on planar samples (3 or $6 \mu\text{m}$) using a polarising optical microscope (Nikon Eclipse). Cells were prepared from glass plates provided with transparent ITO electrodes with area of $5 \times 5 \text{ mm}^2$. The glasses were glued together and mylar sheets were used as spacers. The cells were filled in the isotropic phase. Temperature was stabilised with accuracy $\pm 0.1^\circ\text{C}$ in the hot stage (Linkam) placed on the table of polarising optical microscope. For some optical measurements (birefringence measurements and observation of Williams domains), commercial cells provided with aligning layers were used. Free-standing films were prepared by spreading melted material over a circular hole in a metal plate.

Frequency dispersion of dielectric permittivity was measured on cooling using a Schlumberger 1260 impedance analyser in the frequency range 1 Hz–1 MHz, keeping the temperature of the sample stable during frequency sweeps within $\pm 0.1 \text{ K}$. The frequency dispersion data were analysed using the Cole–Cole formula for the frequency dependent complex permittivity complemented by second and

third terms to eliminate the low-frequency contribution from dc conductivity, σ , and the high-frequency contribution due to resistance of the ITO electrodes, respectively:

$$\varepsilon^* - \varepsilon_\infty = \frac{\Delta\varepsilon}{1 + (if/f_r)^{(1-\alpha)}} - i\left(\frac{\sigma}{2\pi\varepsilon_0 f^n} + Af^m\right), \quad (1)$$

where f_r is the relaxation frequency, $\Delta\varepsilon$ the dielectric strength, α the distribution parameter of relaxation, ε_0 the permittivity of a vacuum, ε_∞ the high-frequency permittivity and n , m , A are fitting parameters. Measured real, ε' , and imaginary, ε'' , parts of the dielectric permittivity, $\varepsilon^*(f) = \varepsilon' - i\varepsilon''$ were simultaneously fitted to Equation (1).

Birefringence was measured with a setup based on a He-Ne laser, photoelastic modulator (Hinds PEM-90), lock-in amplifier (EG&G 7265) and photodiode (FLCE PIN20), for light propagating along the normal to the cell surface. Second harmonic generation (SHG) measurements were performed using a Q-switched Nd-YAG laser (6 ns pulses at 20 Hz, $\lambda = 1064$ nm). The sample was turned 45° with respect to the beam direction and the fundamental wave had p-polarisation. The SH signal at 532 nm was detected by a photomultiplier and boxcar averager. To avoid sample damage very weak pulses (<0.1 mJ) were used, without any focusing. A spot of 1 mm diameter allowed investigation of the average signal from the observed texture.

Smectic layer spacing was measured by small-angle X-ray diffraction measurements using a Bruker Nanostar diffractometer equipped with heating stage allowing a temperature control with the precision of 0.1 K. Experiments were done in the transmission mode for samples prepared in Lindemann capillaries.

3. Results

Calorimetric studies

For all compounds, DSC studies were performed and the phase transition temperatures and associated enthalpy changes collected in Table 1. For all studied compounds, except of **If**, at least two mesophases were observed. For **If**, direct crystallisation takes place on cooling from the isotropic phase. Identification of phases and their properties are described below. In Figures 1(a) and 1(b), DSC thermograms are shown for two selected compounds. In the inset of Figure 1, phase transitions accompanied with a low enthalpy are shown in an enlarged scale. Melting and clearing temperatures are lower for CH_3 -substituted compounds **Ib** and **Ic** in comparison with non-substituted **Ia**.

Texture observation and application of electric field

The nematic phase was established for all studied compounds except for non-mesogenic **If**. The characteristic schlieren texture was observed in this phase in planar samples under a polarising optical

Table 1. Melting point, m.p., detected on second heating, phase transition temperatures, T_{tr} , and the temperature of crystallisation, T_{cr} , detected on second cooling at a rate of 5 K min^{-1} , and corresponding enthalpies, ΔH , in kJ mol^{-1} .

Comp.	X	Y	R ₁	R ₂	m.p./°C	ΔH	T_{cr} /°C	ΔH	SmC ₂	T_{tr} /°C	ΔH	SmC ₁	T_{tr} /°C	ΔH	N	T_{tr} /°C	ΔH	I
Ia	H	H	C ₁₂ H ₂₅	C ₁₂ H ₂₅	143	+51.0	128	-40.1	–	–	–	•	173	-1.23	•	–	187	•
Ib	CH ₃	H	C ₁₂ H ₂₅	C ₁₂ H ₂₅	138	+30.8	131	-29.6	–	–	–	•	164	-0.69	•	–	178	•
Ic	H	CH ₃	C ₁₂ H ₂₅	C ₁₂ H ₂₅	123	+35.5	103	-30.1	•	120	-0.02	•	152	-0.58	•	–	171	•
Id	H	CH ₃	C ₁₀ H ₂₁	(CH ₂) ₉ CH=CH ₂	133	+49.4	103	-32.6	•	140	-0.15	•	147	-0.08	•	–	175	•
Ie	H	Cl	C ₁₀ H ₂₁	(CH ₂) ₉ CH=CH ₂	130	+46.3	109	-30.5	•	133	-1.55	–	–	–	•	–	144	•
If	H	CN	C ₁₀ H ₂₁	(CH ₂) ₉ CH=CH ₂	152	+34.1	146	-16.02	–	–	–	–	–	–	–	–	–	•

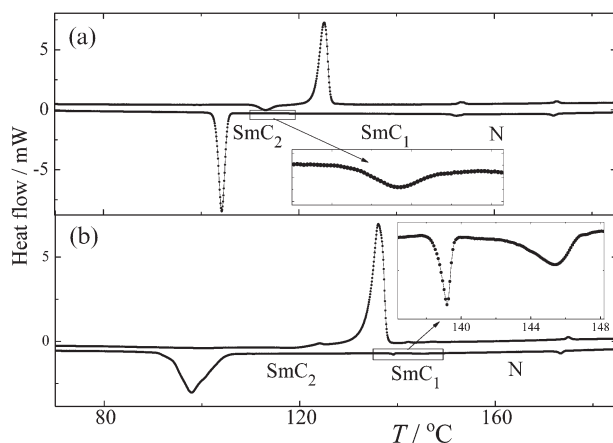


Figure 1. DSC plots for compounds (a) **1c** and (b) **1d**. The upper curve shows the second heating run, the lower curve corresponds to the subsequent cooling; phases are as designated. In the insets the part within the demarked rectangles are enlarged in the vicinity of the SmC_1 - SmC_2 phase transitions.

microscope (see Figure 2(a)). The colour of the schlieren texture changes with temperature (cf. the next paragraph for birefringence). In the commercial cell with surfactant, the aligned planar texture occurs with the extinction position oriented along the rubbing direction. In such a cell, Williams domains (53) occur as a stripe patterns in the nematic phase (vide infra, Figure 4) subjected to a dc electric field with a threshold of about $10 \text{ V } \mu\text{m}^{-1}$. The stripes are oriented perpendicular to the rubbing direction.

For non-substituted compound **1a** and compounds **1b**, **1c** and **1d** with a lateral substitution of the naphthalene by CH_3 group, a tilted smectic phase (SmC_1) has been observed below the nematic phase with typical fan-shaped texture. Across the fans large irregular domains are superimposed with boundaries preferentially directed along the smectic layers (Figure 2(b)). The position of the optical extinction of neighbouring domains is inclined by about 20° to

opposite directions from the smectic layer normal. We conclude that this phase has the synclincic SmC structure.

CH_3 -substituted compounds **1c** and **1d** exhibit a phase transition to another smectic phase on cooling (SmC_2), both phases coexisting in a very narrow temperature interval (see Figure 2(c)). Figure 2(d) shows the texture of the low-temperature phase, composed of fans with stripes parallel to layer orientation. The extinction position in this phase is parallel to the layer normal, which suggests the anticlinic arrangement in the next smectic layers.

Free-standing films of **1d** have been observed in the temperature regions of both smectic phases. In the SmC_1 phase, a typical schlieren texture of the SmC structure is observed with $\pm 2\pi$ wedge disclinations (54), confirming the synclincic structure. In the SmC_2 phase, apart from $\pm 2\pi$ disclinations, $\pm \pi$ disclinations were also found. When observing between crossed polarisers, these disclinations are seen as points from which four or two dark brushes come out for $\pm 2\pi$ or $\pm \pi$ disclination, respectively (54). The position of brushes is rotated when rotating the polarisers keeping them crossed (Figure 3). The existence of $\pm \pi$ disclinations in the SmC_2 phase definitely confirms its anticlinic structure (55).

Application of a dc electric field did not lead to any change of extinction up to a field value of about $40 \text{ V } \mu\text{m}^{-1}$. Nevertheless, when increasing the field strong flow instabilities occur (see Figure 4), which cease at a critical field of about $20 \text{ V } \mu\text{m}^{-1}$. Under an ac electric field with triangular voltage shape, the current profile shows a distinct peak (see Figure 5) in the field region where the instabilities occurs. This peak has different shape and height in various samples and may be found even in the nematic phase. When lowering the temperature it becomes significantly lower, vanishing in the SmC_2 phase. An

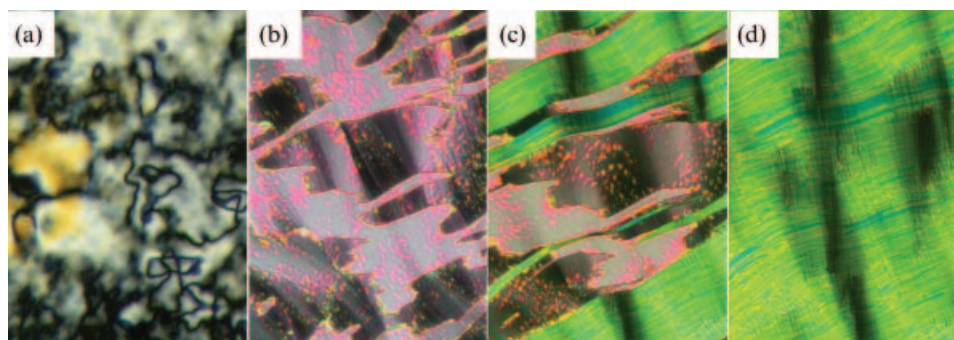


Figure 2. Planar texture of **1c** in the (a) nematic phase at $T=160^\circ\text{C}$, (b) SmC_1 phase at $T=125^\circ\text{C}$, (c) at the SmC_1 - SmC_2 phase transition ($T=120^\circ\text{C}$) and (d) SmC_2 phase at $T=115^\circ\text{C}$.

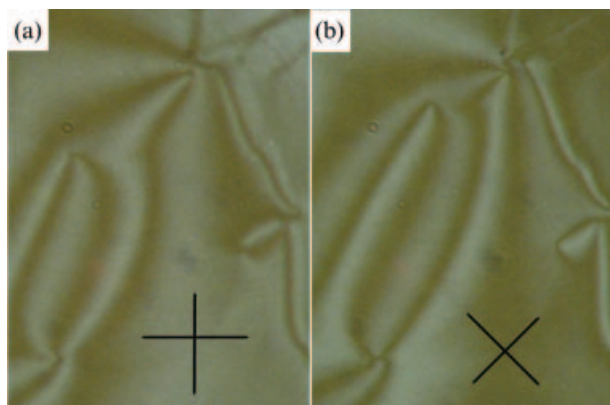


Figure 3. Free standing films of **1d** observed in the SmC₂ phase between crossed polarisers. The orientation of the polarisers is shown in each figure. Width of the picture is about 100 μm .

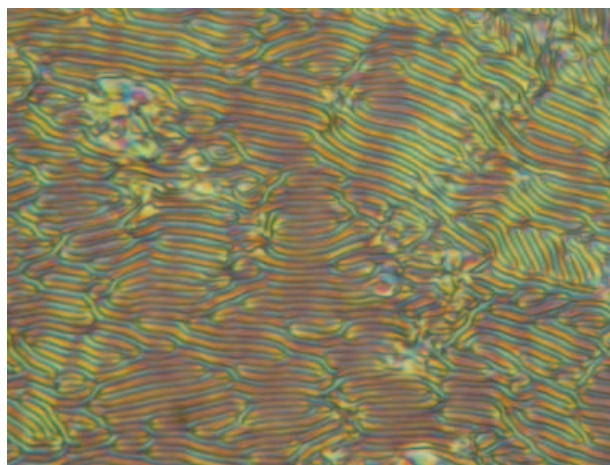


Figure 4. Planar texture in the nematic phase of compound **1d** under a dc electric field of about $20 \text{ V}\mu\text{m}^{-1}$. Width of the picture is about $150 \mu\text{m}$, temperature $T=160^\circ\text{C}$.

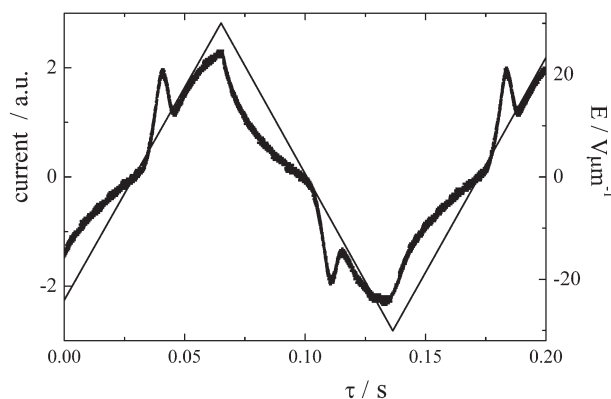


Figure 5. Switching current profile taken at frequency of about 8 Hz for **1b** compound in the SmC₁ phase $T=150^\circ\text{C}$.

electric field up to $40 \text{ V}\mu\text{m}^{-1}$ did not induce switching between different states corresponding to opposite field polarity, so banana anticlinic order can be excluded.

Optical properties: birefringence and SHG measurements

Birefringence was measured for compounds **1c** and **1d** and its temperature dependence is shown in Figure 6.

A significant increase of birefringence is seen within the nematic phase on cooling, coming from the increase of the nematic order. Jumps of the birefringence occur at the phase transitions, which are responsible for the large optical contrast between the phases (Figure 2(c)) SHG measurements were also performed for compounds **1c** and **1d**. Figure 7 shows the profile of the SHG signal in dependence on the applied electric field for two distinct temperatures in the SmC₁ and the SmC₂ phase.

X-ray measurements

From small-angle X-ray diffraction measurements, the layer spacing was evaluated. The results for compounds **1c** and **1d** are shown in Figures 8. For **1d** a small broad peak is detected in this diffraction angle

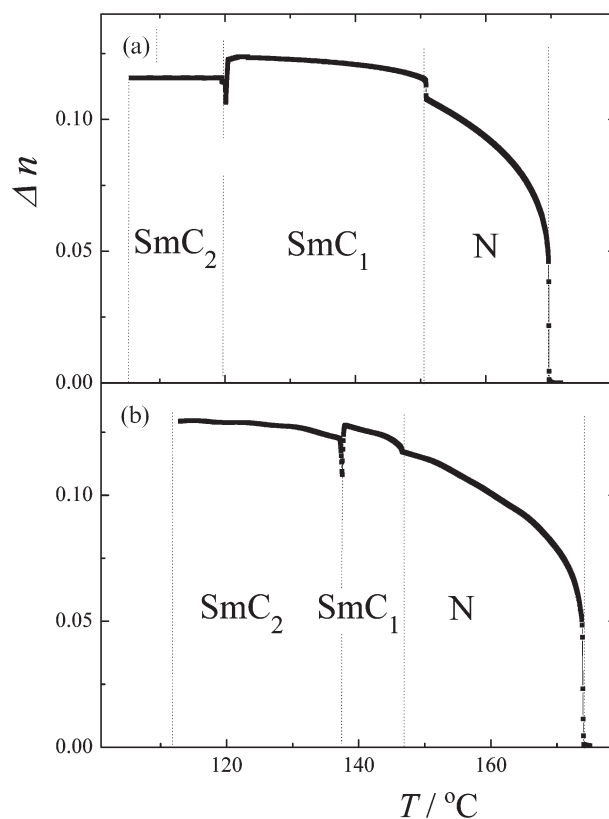


Figure 6. Temperature dependence of the birefringence for compound (a) **1c** and (b) **1d**. Phases are designated.

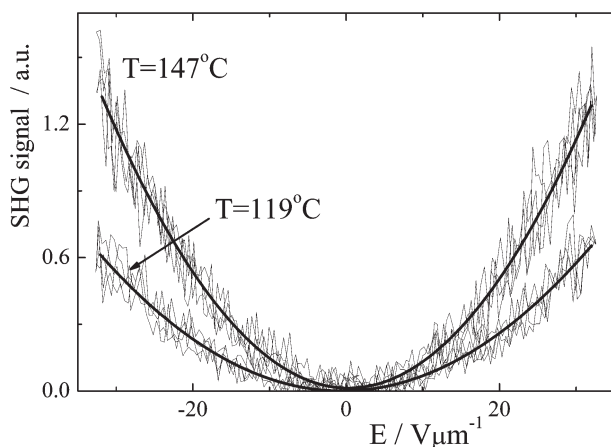


Figure 7. SHG signal for compound **1c** in the SmC_1 phase ($T=147^\circ\text{C}$) and the SmC_2 ($T=119^\circ\text{C}$). The thick solid lines are parabolic fits.

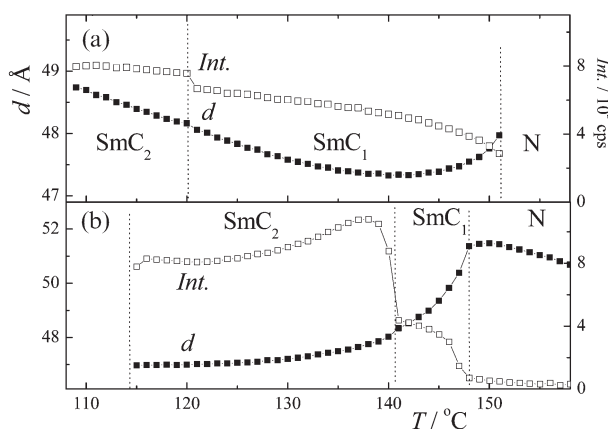


Figure 8. Temperature dependences of the layer spacing (full symbols) and intensity of X-ray signal (empty symbols) for compound (a) **1c** and (b) **1d**. Phases are designated in corresponding temperature intervals. Points in nematic phase represent a short-range pre-translational smectic ordering.

range even in the nematic phase. Its intensity is small and slightly increases when approaching the SmC phase on cooling. This indicates pre-translational smectic ordering above the SmC phase. The periodicity calculated from this ordering is increased on cooling. For the other studied compounds, the smectic-like ordering in the nematic phase is much smaller and could not be detected. The diffracted intensity, expressing the evolution of the smectic ordering, increases within the smectic phases on cooling and jumps up at the SmC_1 – SmC_2 phase transition. For **1d** the layer spacing, d , decreases continuously on cooling through the smectic phases; for **1c** it starts to increase about 10 K below the nematic phase. In both cases there is practically no anomaly at the SmC_1 – SmC_2 phase transition.

In the short-angle diffraction region, no peak in diffracted intensity is detected, which proves that no in-plane ordering exists in both observed smectic phases.

Dielectric spectroscopy

Dielectric spectroscopy reveals one distinct relaxation mode in each mesophase and a contribution to the permittivity from the conductivity, which appears at low frequencies and is much higher at high temperatures. The results are presented as three-dimensional graphs in Figure 9 and 10 for compounds **1c** and **1d**, respectively.

Using the Cole–Cole formula with subtraction of the conductivity contribution, the relaxation frequency, f_r , and dielectric strength, $\Delta\epsilon$, were determined by fitting the experimental data. The conductivity contribution is much higher at high temperatures. The results of fitting are shown in Figure 11 for **1c** and **1d**. The relaxation frequency decreases continuously on cooling across all mesophases, without any anomaly at the phase transition. This suggests that the relaxation is connected with a non-collective (molecular) mode, highly probably with the rotation of molecules around their long axis. The very low $\Delta\epsilon$ of this mode supports this idea. The anomalies in $\Delta\epsilon$ at the phase transitions are probably connected with reorientation of molecules.

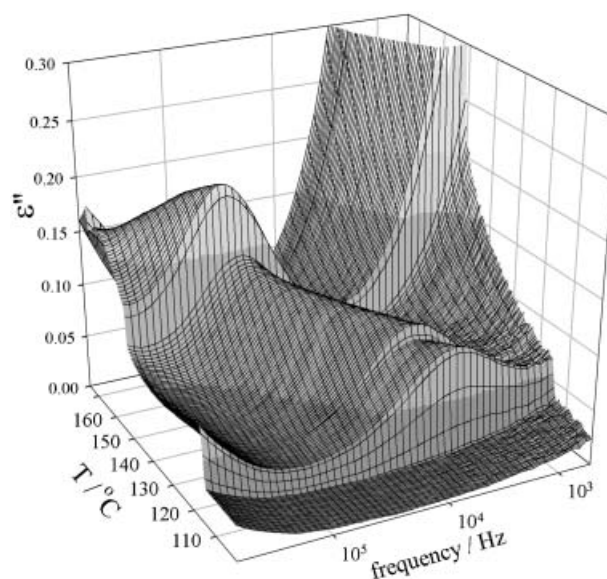


Figure 9. Three-dimensional plot of the imaginary part of the dielectric permittivity for compound **1c**.

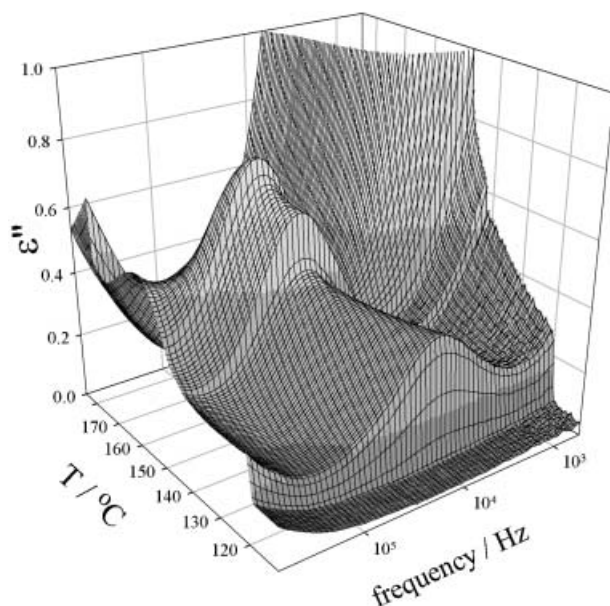


Figure 10. Three-dimensional plot of the imaginary part of the dielectric permittivity for compound **1d**.

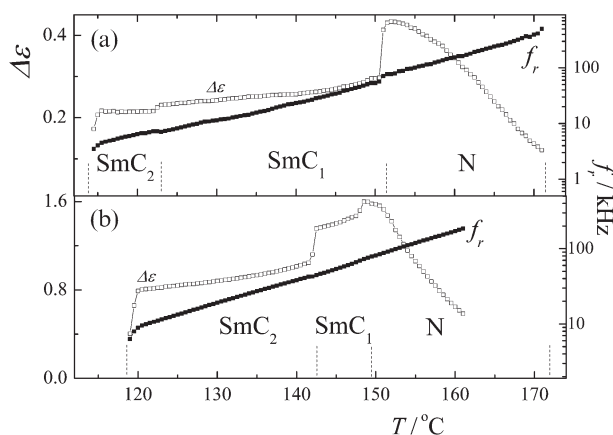


Figure 11. Fitted values of the dielectric strength and relaxation frequency of a mode detected in the temperature interval of the nematic, SmC₁ and SmC₂ phase on cooling from the isotropic phase for compounds (a) **1c** and (b) **1d**.

4. Discussion and conclusions

A new series of six hockey-stick materials composed of five benzene rings connected by ester linking groups with identical orientation was studied. The shorter arm is represented by one benzene ring with an alkoxy tail ($-\text{OC}_{10}\text{H}_{21}$ or $-\text{OC}_{12}\text{H}_{25}$); the longer arm was created from three benzene units and the terminal tail was chosen to be dodecyl and undecenyl as a model of monomer for polymeric liquid crystals. Introduction of non-symmetrical arms to the molecular structure leads to appearance of polymorphism in comparison with the related symmetrical bent-shaped materials reported previously (22, 23, 47), in

which only one typical banana mesophase was observed for every compound and strong dependence of mesomorphic properties on the type of substitution on the naphthalene core was found. On the other hand, the temperature interval of mesomorphic behaviour is almost preserved. The central naphthalene ring was also modified by lateral substituents (methyl, chloro and cyano). In analogy to the related bent-shaped materials studied previously (22, 23, 47), the type of lateral substituent influences formation of various mesophases. Nevertheless, the hockey-stick materials **1a–1e** presented here behave like common rod-like materials with a large anisotropy in spite of their bent structure.

With the exception of the cyano-substituted mesogen (**1f**), which did not exhibit any mesomorphic properties, the other materials (**1a–1e**) formed of at least two mesophases. All compounds exhibited a nematic phase; the non-substituted compound (**1a**) as well as the methyl-substituted compound (**1b**) exhibit one smectic mesophase (SmC₁). When the methyl substitution is moved on the naphthalene core to a position closer to the longer arm (**1c**), two smectic phases occurs (SmC₁ and SmC₂), which persist even when the long arm is modified (**1d**). The SmC₂ phase occurs even when the naphthalene core is substituted by Cl (**1e**).

According to X-ray results, both SmC₁ and SmC₂ phases exhibit no ordering in the smectic layers. In the SmC₁ phase the tilt in the smectic layers has been evaluated. These facts together with the typical fan-shaped texture allow us to establish these phases as tilted smectic C phases, the upper having synclinc molecular orientation. The low-temperature SmC₂ phase exhibits extinction parallel to the layer normal, which suggests an anticlinic alignment. The anticlinic order has been confirmed by finding $\pm\pi$ disclination in free-standing films. Formation of two tilted SmC phases below the nematic phase is the most surprising result of these experimental studies. The same phase sequence has also been found (44) for a compound with molecules of hockey-stick shape.

In the SmC₁ phase, a peak has been found in the response current taken under a triangular wave of electric field. This peak may be found even in the nematic phase, being significantly lower in the low-temperature phases. We suppose that this peak does not correspond to polarisation switching, but to ionic current, similar to that reported by Yu and Yu (44). The dielectric spectroscopy data (Figures 9–10) confirm the significant lowering of the current at low temperatures. The results of the SHG also confirm that both smectic phases have a non-polar symmetry.

It can be concluded that despite of the hockey-stick (bent) molecular shape the studied compounds behave

like common rod-like materials. Both synclinic SmC_1 and anticlinic SmC_2 phases do not exhibit dipolar order. In non-chiral materials, dipolar order could appear only when banana packing of molecules occurs.

Acknowledgements

This work was supported by Research Project AVOZ 10100520, Grant Agency of AS CR (project No. IAA100100710) and Ministry of Education, Youth and Sports of the Czech Republic (project OC176). The X-ray diffraction measurements were accomplished at the Structural Research Laboratory, Chemistry Department, University of Warsaw, Poland, which has been established with financial support from European Regional Development Fund, project no: WKP 1/1.4.3./1/2004/72/72/165/2005/U.

References

- Pelzl G.; Diele S.; Weissflog W. *Adv. Mater.* **1999**, *11*, 707–724, and references cited therein.
- Weissflog W.; Nádasi H.; Dunemann U.; Pelzl G.; Diele S.; Eremin A.; Kresse H. *J. Mater. Chem.* **2001**, *11*, 2748–2758, and references cited therein.
- Dunemann U.; Schröder M.W.; Amarantha Reddy R.; Pelzl G.; Diele S.; Weissflog W. *J. Mater. Chem.* **2005**, *15*, 4051–4061, and references cited therein.
- Amarantha Reddy R.; Tschierske C. *J. Mater. Chem.* **2006**, *16*, 907–961, and references cited therein.
- Takezoe H.; Takanishi Y. *Jap. J. Appl. Phys.* **2006**, *45*, 597–625.
- Pelzl G.; Diele S.; Jákli A.; Weissflog W. *Liq. Cryst.* **2006**, *33*, 1513–1518.
- Pelzl G.; Diele S.; Jákli A.; Lischka C.; Wirth I.; Weissflog W. *Liq. Cryst.* **2006**, *33*, 1519–1523.
- Kwon S.-S.; Kim T.-S.; Lee C.-K.; Choi H.; Shin S.-T.; Park J.-K.; Zin W.-C.; Chien L.-C.; Choi S.-S.; Choi E.-J. *Liq. Cryst.* **2006**, *33*, 1005–1014.
- Dantlgraber G.; Keith C.; Baumeister U.; Tschierske C. *J. Mater. Chem.* **2007**, *17*, 3419–3426.
- Yelamaggad C.V.; Mathews M.; Nagamani S.A.; Shankar Rao D.S.; Prasad S.K.; Findeisen S.; Weissflog W. *J. Mater. Chem.* **2007**, *17*, 284–298.
- Lee S.K.; Park C.W.; Lee J.G.; Kang K.-T.; Nishida K.; Shimbo Y.; Takanishi Y.T.; Takezoe H. *Liq. Cryst.* **2005**, *32*, 1205–1212.
- Umadevi S.; Sadashiva B.K. *Liq. Cryst.* **2005**, *32*, 1233–1241.
- Umadevi S.; Sadashiva B.K. *Chem. Mater.* **2006**, *18*, 5186–5192.
- Prasad V.; Kang S.-W.; Kumar S. *J. Mater. Chem.* **2003**, *13*, 1259–1264.
- Prasad V.; Kang S.-W.; Qi X.; Kumar S. *J. Mater. Chem.* **2004**, *14*, 1495–1502.
- Shreenivasa Murthy H.N.; Sadashiva B.K. *Liq. Cryst.* **2004**, *31*, 567–578.
- Achten R.; Cuyppers R.; Giesbers M.; Koudijs A.; Marcelis A.T.M.; Sudhölter E.J.R. *Liq. Cryst.* **2004**, *31*, 1167–1174.
- Shreenivasa Murthy H.N.; Sadashiva B.K. *Liq. Cryst.* **2004**, *31*, 1337–1346.
- Shreenivasa Murthy H.N.; Sadashiva B.K. *Liq. Cryst.* **2004**, *31*, 1347–1356.
- Achten R.; Koudijs A.; Giesbers M.; Marcelis A.T.M.; Sudhölter E.J.R. *Liq. Cryst.* **2005**, *32*, 277–285.
- Achten R.; Koudijs A.; Giesbers M.; Amarantha Reddy R.; Verhulst T.; Tschierske C.; Marcelis A.T.M.; Sudhölter E.J.R. *Liq. Cryst.* **2006**, *33*, 681–688.
- Kozmík V.; Kovářová A.; Kuchař M.; Svoboda J.; Novotná V.; Glogarová M.; Kroupa J. *Liq. Cryst.* **2006**, *33*, 41–56.
- Keith C.; Dantlgraber G.; Amarantha Reddy R.; Baumeister U.; Prehm M.; Hahn H.; Lang H.; Tschierske C. *J. Mater. Chem.* **2007**, *17*, 3796–3805.
- Schröder M.W.; Pelzl G.; Dunemann U.; Weissflog W. *Liq. Cryst.* **2004**, *31*, 633–637.
- Prasad V.; Jákli A. *Liq. Cryst.* **2004**, *31*, 473–479.
- Shreenivasa Murthy H.N.; Sadashiva B.K. *Liq. Cryst.* **2004**, *31*, 361–370.
- Amarantha Reddy R.; Sadashiva B.K. *J. Mater. Chem.* **2004**, *14*, 310–319.
- Weissflog W.; Naumann G.; Košata B.; Schröder M.W.; Eremin A.; Diele S.; Vakhovskaya Z.; Kresse H.; Friedemann R.; Ananda Rama Krishnan S., et al. *J. Mater. Chem.* **2005**, *15*, 4328–4337.
- Shreenivasa Murthy H.N.; Sadashiva B.K. *J. Mater. Chem.* **2005**, *15*, 2056–2064.
- Novotná V.; Kašpar M.; Hamplová V.; Glogarová M.; Lejček L.; Kroupa J.; Pocięcha D. *J. Mater. Chem.* **2006**, *16*, 2031–2038.
- Shreenivasa Murthy H.N.; Sadashiva B.K. *J. Mater. Chem.* **2004**, *14*, 2813–2821.
- Achten R.; Smits E.A.W.; Amarantha Reddy R.; Giesbers M.; Marcelis A.T.M.; Sudhölter E.J.R. *Liq. Cryst.* **2006**, *33*, 57–65.
- Amarantha Reddy R.; Sadashiva B.K.; Baumeister U. *J. Mater. Chem.* **2005**, *15*, 3303–3316.
- Gimeno N.; Blanca Ros M.; Serrano J.L.; de la Fuente M.R. *Angew. Chem. Int. Ed.* **2004**, *43*, 5235–5238.
- Amarantha Reddy R.; Schröder M.W.; Bodyagin M.; Kresse H.; Diele S.; Pelzl G.; Weissflog W. *Angew. Chem. Int. Ed.* **2005**, *44*, 774–778.
- Kovalenko L.; Schröder M.W.; Amarantha Reddy R.; Diele S.; Pelzl G.; Weissflog W. *Liq. Cryst.* **2005**, *32*, 857–865.
- Shreenivasa Murthy H.N.; Bodyagin M.; Diele S.; Baumeister U.; Pelzl G.; Weissflog W. *J. Mater. Chem.* **2006**, *16*, 1634–1643.
- Weissflog W.; Shreenivasa Murthy H.N.; Diele S.; Pelzl G. *Phil. Trans. R. Soc. A* **2006**, *364*, 2657–2679.
- Folcia C.L.; Alonso I.; Ortega J.; Extebarria J.; Pintre I.; Blanca Ros M. *Chem. Mater.* **2006**, *18*, 4617–4626.
- Pintre I.C.; Gimeno N.; Serrano J.L.; Blanca Ros M.; Alonso I.; Folcia C.L.; Ortega J.; Extebarria J. *J. Mater. Chem.* **2007**, *17*, 2219–2227.
- Dingemans T.J.; Murthy N.S.; Samulski E.T. *J. Phys. Chem. B* **2001**, *105*, 8845–8860.
- Das B.; Grande S.; Weissflog W.; Eremin A.; Schröder M.W.; Pelzl G.; Diele S.; Kresse H. *Liq. Cryst.* **2003**, *30*, 529–539.
- Stannarius R.; Li J.; Weissflog W. *Phys. Rev. Lett.* **2003**, *90*, 025502.
- Yu F.C.; Yu L.J. *Chem. Mater.* **2006**, *18*, 5410–5420.
- Cristiano R.; Vieira A.A.; Ely F.; Gallardo H. *Liq. Cryst.* **2006**, *33*, 381–390.

- (46) Svoboda J.; Novotná V.; Kozmík V.; Glogarová M.; Weissflog W.; Diele S.; Pelzl G. *J. Mater. Chem.* **2003**, *13*, 2104–2110.
- (47) Kozmík V.; Kuchař M.; Svoboda J.; Novotná V.; Glogarová M.; Baumeister U.; Diele S. *Liq. Cryst.* **2005**, *32*, 1151–1160.
- (48) Novotná V.; Kohout M.; Svoboda J.; Glogarová M.; Baumeister U., In *Proceedings of the 11th International Conference on Ferroelectric Liquid Crystals*, Hokkaido, Japan, September 3–8, 2007, pp. 1–26.
- (49) Kohout M.; Kozmík V.; Svoboda J.; Glogarová M.; Novotná V., In *Proceedings of the 9th European Conference on Liquid Crystals*, Lisbon, Portugal, July 2–6, 2007, p. 10.
- (50) Heinrich B.; Guillon D. *Mol. Cryst. Liq. Cryst. Sci. Technol. A* **1995**, *268*, 21–43.
- (51) Nozary H.; Piquet C.; Rivera J.-P.; Tissot P.; Morgantini P.-Y.; Weber J.; Bernardinelli G.; Bünzli J.-C.G.; Deschenaux R.; Donnio B., et al. *Chem. Mater.* **2002**, *14*, 1075–1090.
- (52) Kelly S.M.; Buchecker R. *Helv. Chim. Acta* **1988**, *71*, 461–466.
- (53) de Gennes P.; Prost J. *The Physics of Liquid Crystals*; Clarendon Press: Oxford, 1999.
- (54) Demus D.; Richter L. *Textures of Liquid Crystals*; VEB Deutscher Verlag für Grundstoffindustrie: Leipzig, 1978.
- (55) Takanishi Y.; Takezoe H.; Fukuda A. *Phys. Rev. B* **1992**, *45*, 7684–7489.